MAP6-F is a temperature sensor that directly binds to and protects microtubules from cold-induced depolymerization.

Christian Delphin, Denis Bouvier, Maxime Seggio, Emilie Couriol, Yasmina Saoudi, Eric Denarier, Christophe Bosc, Odile Valiron, Mariano Bisbal, Isabelle Arnal, et al.

MAP6-F is a temperature sensor that directly binds to and protects microtubules from cold-induced depolymerization*

Christian Delphin[1§], Denis Bouvier[2], Maxime Seggio[1], Emilie Couriol[1], Yasmina Saoudi[1], Eric Denarier[1], Christophe Bosc[1], Odile Valiron[1], Mariano Bisbal[1], Isabelle Arnal[3] and Annie Andrieux[1]

[1]From the Institut National de la Santé et de la Recherche Médicale, U836-GIN team 1 « Physiopathology of Cytoskeleton »; Commissariat Energie Atomique, iRTSV-GPC; Site Santé La Tronche, BP170, 38042 Grenoble, Cedex 9, France

[2] Grenoble Outstation, European Molecular Biology Laboratory, 6 rue Jules Horowitz, BP181, 38042 Grenoble Cedex 9, France.

[3] Institut National de la Santé et de la Recherche Médicale, U836-GIN, team 13 « Dynamic and structural regulation of Cytoskeleton », Site Santé La Tronche, BP170, 38042 Grenoble, Cedex 9, France

*Running title: Microtubule stabilization by MAP6

[§]To whom correspondence should be addressed: Christian Delphin, Inserm U836, Equipe 1 Bâtiment Edmond J. Safra, Université Joseph Fourier, Site Santé à La Tronche , BP 170, 38042 GRENOBLE Cedex 9 – France, Tel: (33)-456-520-539; Fax: (33)-456-520-657; E-Mail: christian.delphin@ujf-grenoble.fr

Keywords: Microtubules; MAP6; hypothermia

Background: Microtubules are intrinsically cold-sensitive polymers but cold-stable microtubules are observed in cells.

Results: Progressive temperature-dependent conformational change in MAP6-F coincides with its binding to microtubules and with its microtubule cold stabilization activity.

Conclusion: MAP6-F is a temperature sensor that protects microtubules from cold-induced depolymerization at temperatures ranging from 4 to 20°C.

Significance: This work provides a better understanding of cellular microtubule stabilization under hypothermic stress.

SUMMARY

Microtubules are dynamic structures that present the peculiar characteristic to be ice-cold-labile *in vitro*. *In vivo*, microtubules are protected from ice-cold induced depolymerization by the widely expressed MAP6/STOP family of proteins. However, the mechanism by which MAP6 stabilizes microtubules at 4°C has not been identified. Moreover, the microtubule cold sensitivity and therefore the needs for microtubule stabilization in the wide range of temperatures between 4 and 37°C are unknown. This is of importance as body temperatures of animals can drop during hibernation or torpor covering a large range of temperatures. Here, we show that in the absence of MAP6, microtubules in cells below 20°C rapidly depolymerize in a temperature-dependent manner whereas they are stabilized in the presence of MAP6. We further show that in cells, MAP6-F binding to- and stabilization of microtubules is temperature dependent and very dynamic, suggesting a direct effect of the temperature on the formation of microtubule/MAP6 complex. We also demonstrate, using purified proteins, that MAP6-F binds directly to microtubules through its Mc domain. This binding is temperature-dependent and coincides with progressive conformational changes of the Mc domain as revealed by circular dichroism. Thus, MAP6 might serve as a temperature sensor adapting its conformation according to the temperature to maintain the cellular microtubule network in organisms exposed to temperature decrease.

Microtubules are essential components of the cell cytoskeleton, being involved in cell division, cell migration and intracellular trafficking. Microtubules result from the polymerization of tubulin dimers in protofilaments that associate through lateral contacts (for reviews see (1-4)). Microtubules are dynamic structures alternating growing and shrinking phases ended by catastrophes and rescues, respectively. *In vitro*, microtubule dynamics are under the control of the tubulin concentration and numerous other physico-chemical parameters (5-8). Among them, temperature plays a crucial role as microtubules depolymerize upon a temperature shift from 37°C to 4°C. This could be due to the modification of different dynamics parameters especially the increase of catastrophe and the disappearance of rescue events at such temperatures (9,10). In a cold environment ectothermic organisms express tubulin variants able to assemble at temperatures below 4°C and to resist to cold-induced depolymerization (11). The amino acid substitutions affect residues located at sites implicated in tubulin lateral contact and are thought to increase interactions between protofilaments (12). Among endotherms that contain cold-sensitive microtubules, some may undergo significant drop in their body temperature during natural events. Indeed, during hibernation or torpor, body temperature can decrease by several degrees down to temperatures close to 0°C depending on the species (13,14). In human, deep hypothermia can occur during accidental events or be medically provoked to preserve tissues. During such events, the maintenance of a minimal network of microtubules is thought to be required for basal cellular functions. It has been shown that the main proteins able to protect microtubules against cold-induced depolymerization are the microtubule-associated proteins MAP6 (also called STOP for Stable Tubule Only Polypeptide) (15,16). MAP6 belongs to a family of proteins encoded by a single gene (16,17). They are restricted to vertebrates and expressed in several tissues including brain, heart, muscle, kidney, lung and testis (18). At the cellular level, MAP6 have been found in neurons, astrocytes, oligodendrocytes, fibroblasts and pulmonary endothelium (16,19-21). Depending on mouse strains, MAP6 isoforms contain a Mc domain composed of a 4 or 5 times tandemly-repeated 46 residues motif. This Mc domain, when overexpressed in HeLa cells (that do not express any MAP6 variants), is able to stabilize microtubules against exposure to 4°C (22).

In a previous study, it was shown that NIH/3T3 fibroblastic cells (16) mainly expressed the smallest MAP6-F isoform. In these cells, at 37°C, microtubules are dynamic, non stable (as revealed by nocodazole sensitivity) (23) whereas they are stable at 4°C. Concomitantly, MAP6-F relocalizes from the cytosol at 37°C to the microtubule network upon chilling at 4°C (16). These data suggest that microtubule stabilization by MAP6-F is dependent on the binding of MAP6-F to the microtubules. However, the cold-sensitivity of cellular microtubules to temperatures between 37 and 4°C and the effect of these temperatures on MAP6 binding to microtubules were unclear. Moreover, the exact mechanisms involved in the regulation of MAP6 interaction with microtubules under cold exposure have yet to be identified.

Here, we show that in the absence of MAP6, cellular microtubules depolymerize in a temperature-dependent manner as soon as the temperature decreases below 20°C. In fibroblasts, which contain MAP6-F, microtubule cold resistance is directly correlated with a rapid and temperature-dependent interaction of MAP6-F with the microtubules. Using purified *in vitro* systems, we provide evidence that MAP6-F stabilizes microtubules *via* a direct interaction through its Mc domain. Furthermore, we found structural changes in the MAP6 Mc domain upon temperature modifications, indicating that MAP6 behaves as a "temperature-sensor" adapting its conformation to allow microtubule binding and preservation upon temperature drop.

EXPERIMENTAL PROCEDURES

Cell culture–Mouse fibroblastic NIH/3T3 cells were grown at 37°C in DMEM 4.5 g/L glucose (Gibco BRL) supplemented with 10% foetal bovine serum (Hyclone Laboratories Inc.), 50 U/ml of penicillin and 50 µg of streptomycin (Gibco BRL). Human epithelial HeLa cells and mouse embryonic fibroblasts (MEF) prepared from either wild-type or MAP6-null mice as in (24), were maintained as for NIH/3T3 cells except that 1 g/L glucose DMEM was used instead of 4.5 g/L glucose DMEM.

Cell cold treatment and permeabilization–For immunofluorescence analysis of cellular microtubule content, cells were plated 24 to 48 h before analysis on glass coverslips placed in B60 cell culture dishes. For analysis of time- and temperature-dependent effects on cellular

microtubule content, coverslips were placed in culture medium complemented with 10 mM HEPES pH 7.4 in P24 culture dishes whose temperature was pre-equilibrated in water baths. For short incubation times of 1 min or less, incubations were done in PBS instead of culture medium. At the end of the indicated time, cells were washed with PBS at the incubation temperature and then permeabilized to wash out the soluble cell content through two 30 seconds incubations in OPT buffer (100 mM PIPES/KOH pH 6.75, 1 mM $MgCl_2$, 1 mM EGTA, 10 % glycerol, 0.5 % Triton X-100) at the incubation temperature. Cells were then fixed in -20°C methanol and processed for immunodetection. For immunofluorescence analysis of MAP6-dependent microtubule cold stability, NIH/3T3 cells on coverslips were treated as described above except that cells were permeabilized and washed (2 x 30 s) in PEMT buffer (OPT buffer without glycerol) at the incubation temperature and then dipped in 4°C PEMT buffer for 10 min before methanol fixation.

Detection and quantification of cellular microtubule content by immunofluorescence– Methanol-fixed cells were incubated for 30 min in PBST (PBS buffer plus 0.3% Tween20) plus 5% (v/v) of normal goat serum (NGS). Mouse monoclonal anti-tubulin α3a1 antibody (24) (dilution 1/6000) in PBST plus 1% NGS was then added and incubated for 1 h at room temperature. Coverslips were washed 5 times with PBST and then incubated for 45 min with Alexa488-coupled anti-mouse secondary antibody (Invitrogen). Coverslips were washed 5 times with PBST, once with PBS, incubated for 15 min with PBS containing 100 ng/ml of Hoechst 33258, briefly rinsed with PBS, ethanol dried and mounted on glass slides using DAKO mounting medium. Images were acquired using Axioskop 50 (Carl Zeiss Micro Imaging) microscope and Metamorph (Universal Imaging Corp., USA) software. For microtubule quantification, at least 12 pictures of 30 to 50 cells were taken for each condition. The surface covered by microtubules was quantified using ImageJ software (25) and reported to the number of cells in each corresponding picture. Statistical analysis and graphs were made using Excel software (Microsoft).

Immunofluorescence analysis of MAP6-F association with the microtubule network.
MEF cells grown on coverslips were placed in culture medium complemented with 10 mM HEPES pH 7.4 and either kept at 37°C or incubated at 4°C for 30 min. Cells were permeabilized in OPT buffer and fixed with 3.7% paraformaldehyde, 0.5% glutaraldehyde, and 0.1% Triton X-100 in PBS, followed by a treatment with 1 mg/ml NaBH4 in PBS for 10 min. Tubulin was detected using a3A1 antibody (1/1000) and MAP6-F with polyclonal 23C antibody (1/1000). Images were recorded with an Axioskop 20 microscope (Carl Zeiss) (Leica) coupled with Coolnaps ES camera (Roper Scientific) driven by Metaview Software (Universal Imaging).

Video microscopy analysis of mCherry-MAP6-F localization in HeLa Cells.
pmCherry-C2 vector was obtained by replacing the EGFP sequence of pEGFP-C2 vector (Clontech) by the mCherry sequence from pmCherry-C1 (Clontech) using AgeI/BsrG1 coloning sites. mCherry-MAP6-F expression vector was then constructed by inserting MAP6-F cDNA from p16C-APa (16) into pmCherry-C2 vector using XhoI/KpnI cloning sites. HeLa cells transfected with pmCherry-MAP6-F using Amaxa technology (Lonza) were grown on coverslip for 24 hours and then placed in a perfusion chamber at 37°C. Cell culture medium was progressively cooled from 37°C to 15°C during the course of the experiment (15 min). Images were recorded every minute with a DMI6000 microscope (Leica) coupled with EMCCD Quantem camera (Roper Scientific) driven by MetaMorph Software (Universal Imaging).

Western blot analysis of MAP6-F recruitment to cellular insoluble material–For analysis of the temperature-dependent solubility of MAP6-F in NIH/3T3 cells, cells were grown in B35 cell-culture dishes. The cell culture medium was renewed with the same medium supplemented with 10 mM HEPES pH 7.4, equilibrated at the temperature of the assay and the culture dishes were placed in a temperature-controlled water-bath. For incubation times of 1 min or less, PBS was used instead of cell culture medium. Dishes were incubated in water-bath at the temperature and for the time indicated. Dishes were rinsed with 1 ml of PBS at incubation temperature and permeabilized with 400 µl of OPT at the incubation temperature. After 1 min, OPT medium was recovered and added to 100 µl of 5x Leammli buffer (Soluble extract). Insoluble cell material was recovered in 500 µl of 1x Leammli buffer. Extracts were run on 12% SDS-PAGE and transfered onto nitrocellulose membranes. Membranes were blocked with 5% non-fat milk

in TTBS (50mM Tris-HCl pH 7.4, 150 mM NaCl, 0.3% Tween 20). Membranes were probed in the same buffer with affinity purified rabbit anti-MAP6 antibody 23C (dilution 1/5000) or monoclonal anti-tubulin antibody α3a1 (1/10000). HRP-coupled secondary antibodies were incubated in TTBS and probed using Pierce ECL Substrate (ThermoScientific) and light sensitive film (Fischer Scientific).

Western blot Analysis of MAP6 expression in NIH/3T3, HeLa, MEF$^{+/+}$ and MEF$^{-/-}$–Cells grown on B30 cultures dishes were washed with PBS and lyzed by addition of 400 µl of Leammli buffer. Extracts were normalized for the quantity of tubulin by semi-quantitative Western blot using α3A1 antibody. MAP6 proteins expression were then analyzed by Western blot as described above using a mixture of both anti-MAP6 23N and 23C polyclonal antibodies at 1/5000 dilution each.

MAP6-F and Mc domain expression and purification–MAP6-F was cloned into pFAST-BAC HTb as previously reported (22). The Mc domain coding sequences were cloned into Nco I/Xho I cloning sites of pFAST-BAC HTb in frame with the 6xHis tag. Recombinant baculoviruses were obtained and amplified in Sf9 insect cells (Invitrogen). Protein expressions were carried out in High Five insect cells grown in suspension in Express Five culture medium (Invitrogen). For 6His-MAP6-F purification, 500 ml of infected High Five cell culture were spined down at 4°C for 5 min at 125 x *g*. Pellets were frozen and thawed in 50 ml of lysis buffer (20 mM PIPES-KOH pH 6.6, 150 mM KCl, 0.1% Triton X-100, 10% glycerol, 1 mM $MgCl_2$, 1 mM EGTA 0.1 mM DTT, 50 µg/ml AEBSF, 5 µg/ml aprotinin, 10 µg/ml leupeptin, 2.5 µg/ml pepstatin and 10 µg/ml E64. Cells were lyzed by passing three times through a 23G needle and cell debris were pelleted by centrifugation for 30 min at 4°C and 30,000 x *g*. Supernatant was diluted with one volume of Q-Sepharose adjusting buffer (100 mM HEPES pH 8.0, 50 mM KCl, 0.9% Triton X-100, 1 mM EGTA, 1 mM $MgCl_2$ 0.1 mM DTT plus protease inhibitors and centrifuged at 100,000 x *g*. The supernatant was loaded onto a 25 ml Q-Sepharose column equilibrated in Q buffer (100 mM HEPES-KOH pH 8.0, 100 mM KCl, 0.5% Triton X-100, 1 mM EGTA, 1 mM $MgCl_2$, 0.1mM DTT). Flow through and 25 ml wash with Q buffer were collected, mixed with 1 volume of Ni-Sepharose adjustment buffer (60 mM imidazole pH 8.0, 900 mM KCl, 0.5% Triton X-100, 20% sucrose, 1 mM $MgCl_2$, 1 mM EGTA, and protease inhibitors) and incubated at 4°C for 90 min with 1 ml of Ni-Sepharose beads previously equilibrated in Ni column buffer (50 mM HEPES-KOH pH 8.0, 500 mM KCl, 0.5% Triton X-100, 10% sucrose, 50 mM Imidazole, 0.1 mM DTT). Beads were spined down at 100 x *g* for 5 min at 4°C, washed twice with Ni-column buffer and packed in a disposable plastic column. The column was further washed with Ni-column buffer, equilibrated in equilibration buffer (50 mM HEPES-KOH pH8, 250 mM KCl, 0.1 mM DTT, 50 mM Imidazole) and the protein was eluted with equilibration buffer containing 250 mM imidazole. Purified His-MAP6-F was extensively dialyzed against PEM buffer, aliquoted, frozen in liquid nitrogen and stored at -80°C. Protein purity was analyzed on Coomassie blue-stained SDS-PAGE. Quantification was made with ImageJ and Excel softwares from scanned gel using bovine serum albumin as standard. For His-Mc domain purification, a 50 ml culture of infected High Five cells was spined down and frozen as indicated above. Cells were lyzed in 10 ml of buffer (20 mM HEPES pH 7.4, 300 mM NaCl, 0.5% Triton X-100 and protease inhibitors), and centriguged at 30,000 x *g* for 30 min at 4°C. The supernatant was heated at 90°C for 15 min, cooled on ice and centrifuged again. The supernatant was adjusted to 2.5 mM of imidazole and loaded on a 1 ml cobalt column (Pierce) connected to Duo Flow apparatus (BioRad) pre-equilibrated in buffer A (20 mM HEPES pH 7.4, 300 mM NaCl, 2.5 mM imidazole). Column was washed with 20 ml of Buffer A and the proteins were eluted using a 2.5 to 200 mM imidazole gradient. Fractions with the Mc domain were pooled, concentrated with Ultracel-10K (Millipore), loaded on a S200 gel-filtration column equilibrated in 2xBRB buffer (160 mM PIPES pH 6.75, 2 mM EGTA, 2 mM $MgCl_2$). Elution fractions were analyzed, diluted with one volume of water, reconcentrated with Ultracel-10K, aliquoted, frozen in liquid nitrogen and stored at -80°C. For circular dichroism experiments, the buffer containing the Mc domain was changed to 50 mM potassium phosphate buffer (pH 6.75) through repeated concentrations and dilution steps with Ultracel-10K.

In vitro analysis of the Mc domain binding to Taxol-stabilized microtubules-Microtubules were polymerized from 50 µM of brain bovine PC-tubulin prepared as published (26). Tubulin was incubated for 20 min at 37°C in PEM buffer (100

mM PIPES pH 6.75, 1 mM $MgCl_2$, 1 mM EGTA) supplemented with 1 mM of GTP. Mixture was further incubated at 37°C for 10 min in the presence of Taxol (100 µM) and then diluted to 2 µM final concentration of tubulin. Five µl of microtubule solution were incubated with 5 µl of various concentrations of the Mc domain in PEM buffer plus 0.05% Tween20 and 1 mM DTT. After 10 min at the indicated temperature, microtubules were sedimented through centrifugation at 100,000 x *g* for 10 min at the incubation temperature. Pellets were recovered in 80 µl of Leammli buffer. Fifteen µl of each fraction were loaded on a 12% SDS-PAGE gels. After migration, 2 gel bands were cut from each gel. The firsts at 45/60 kDa were Coomassie blue stained to verify the even quantity of tubulin present in the assay. The seconds, at 30-45 kDa were transferred onto a single nitrocellulose membrane at 100 V for 1 h in transfer buffer containing 20% ethanol and 0.05% SDS. The Mc domain detection was carried out as described for Western blot detection of MAP6-F except that pico-ECL kit (Pierce) was used and the signal was recorded with Chemidoc apparatus (BioRad). Signal intensities were quantified with ImageJ software and the corresponding amount of protein present in the extract was determined by comparison with the ECL signal obtained with a ladder of given quantity of the protein using Excel software.

In vitro analysis of microtubules cold-stability-Microtubules were polymerized from 60 µM of bovin brain tubulin in PEM buffer plus 1 µM GTP at 37°C for 30 min. Three µl of microtubule solution were mixed with 3µl of PEM solution containing either 100 µM of taxol or increasing concentration of purified MAP6-F or Mc domain and incubated on ice for 10 min. Five µl of the mix were loaded on 100 µl of a 30% sucrose cushion in PEM buffer, centrifuged at 100,000 x *g* for 30 min at 4°C. The pellets were recovered in Laemmli buffer and analyzed by SDS-PAGE and Coomassie blue staining.

Cryo-electron microscopy analysis of microtubule ends at 4°C–Microtubules were grown from 80 µM of bovine brain tubulin in PEM-GTP buffer for 30 min at 37°C. Microtubules were then diluted at 37°C to 55 µM either with PEM buffer alone or supplemented with the Mc domain (5.5 µM final concentration). After 10 min at 37°C, the mixes were incubated on ice for either 1 min in the control condition (rapid depolymerization) or for 20 min when microtubules were stabilized by the Mc domain. Five µl of chilled mixes were loaded onto holey carbon-coated grids, briefly blotted and plunged into liquid ethan using the vitrification robot Vitrobot MARK IV (FEI company). Specimens were observed with a Phillips CM200 using a Gatan G26 cryoholder. Images were recorded on Kodak SO163 films under low dose conditions at defocus in the range of 2 to 3 µm and at a magnification of 27500 x. Micrographs were digitized with an Epson scanner at 1600 dpi.

Thermostability analysis of MAP6-F–Forty µl of PEM buffer containing 1 µg of MAP6-F were either kept on ice or incubated for 30 min at 90°C. Heated solutions were cooled down on ice and centrifuged at 100,000 x *g* for 15 min at 4°C. Supernatants were recovered and mixed with 10 µl of 5x Leammli buffer, while pellets were resuspended in 50 µl of Leammli buffer. As control for the total amount of MAP6-F, 40 µl of non-centrifuged protein solution were treated as described for the supernatants. Protein solutions were analyzed by SDS-PAGE on 12% gel and Coomassie blue staining.

Circular dichroism analysis–Circular dichroism spectra were recorded with a Jasco J-810 spectropolarimeter interfaced with a Peltier temperature control unit. The Mc domain concentration was 9 µM in 50 mM potassium phosphate buffer at pH 6.75. The path length of the cuvette was 1 mm. Thermal folding was followed by monitoring the CD signal at 220 nm and 208 nm while changing the temperature from 5 to 80°C by 1°C steps. The structural changes observed while varying the temperature was emphasized by subtracting the CD spectrum at 5°C from the CD spectra obtained at given temperatures.

RESULTS

MAP6 protects microtubules against temperature-dependent depolymerization in cells–Previous experiments have shown that in HeLa cells that do not express MAP6 proteins, microtubules depolymerize when incubated on ice for a prolonged time (23). However, no data were available on the effect of moderate chilling conditions on microtubules. To assess the effect of intermediate drops in temperature on cellular microtubules, we incubated HeLa cells grown on coverslips at temperatures varying from 37°C to 4°C before rapid permeabilization and fixation (23). The remaining microtubules were observed

and quantified (Fig.1, *A* and *B*). The quantity of microtubules was constant for temperatures above 25°C. This quantity then progressively decreased with lower temperatures to reach a very low level at 4°C. Similar results were obtained with mouse embryonic fibroblasts derived from MAP6 null mice ($MEF^{-/-}$) (Fig. 1*A* and 1*C*) albeit with stronger chilling effect on microtubules. In $MEF^{-/-}$, significant microtubule loss appeared below 25-20°C with a rapid drop between 20°C and 15°C with only about 20% of microtubule left and a complete microtubule depolymerization below 10°C (Fig. 1*C*).

On the contrary, in NIH/3T3 cells or MEF wild type ($MEF^{+/+}$) that express MAP6, microtubules were mostly resistant to cold-induced depolymerization (Fig. 1*A*). In NIH/3T3 cells, close to 80 % of the total amount of microtubules was preserved at temperatures below 25°C (Fig. 1*B*). In $MEF^{+/+}$, microtubule resistance to cold-induced depolymerization was not as strong as in NIH/3T3 cells, with 80% of remaining microtubules at 15°C and 30% under 10°C (Fig. 1*C*). This discrepancy between NIH/3T3 and $MEF^{+/+}$ could be correlated with the difference of MAP6-F expression as revealed by Western blot analysis (Fig. 1*D*).

We then analyzed the kinetics of cold-induced microtubule depolymerization in HeLa cells that do not express MAP6 proteins at 4°C and 15°C (Fig. 1*E*). At 4°C, microtubules depolymerized rapidly and completely in 2 min. At 15°C, microtubule amount dropped by about 40% in a few minutes but remained stable thereafter. This suggested that, in cells, a decrease in temperature induces a change from an equilibrium state at 37°C to a new one with a lower quantity of microtubules. Altogether, these experiments indicated that below 25-20°C, cellular microtubules depolymerize rapidly in a temperature-dependent manner unless they are protected by the presence of MAP6.

MAP6-F binding to- and stabilization of microtubules under cold exposure are dynamic and temperature-dependent–To better understand the mechanisms involved in microtubule stabilization by MAP6 upon chilling, we intended to correlate the cold conditions required for microtubule depolymerization to those required for MAP6 binding to- and stabilization of microtubules.

It was shown that upon chilling, MAP6-F of NIH/3T3 cells re-localized from the cytoplasm to the microtubule network (16). Cold-dependent association of MAP6-F with microtubules was also observed in $MEF^{+/+}$ as revealed by immunofluorescence analysis (Fig. 2). Indeed, after cell permeabilization, MAP6-F was found associated with the microtubule network at 4°C but not at 37°C (upper panels). The low MAP6-F nuclear labeling visible at 37°C correspond to background as observed in $MEF^{-/-}$ (lower panels). In addition, temperature-dependent translocation of mCherry-MAP6-F from the cytoplasm to microtubules in Hela cells was observed using live video microscopy analysis (Fig. 3). Results revealed a progressive localization of the protein on microtubules during temperature shift from 37°C to 15°C.

To further characterize the association of MAP6-F with microtubules, we performed cell fractionation and analyzed MAP6-F presence in soluble versus insoluble fractions. In parallel, we evaluated MAP6-F activity in NIH/3T3 cells by quantifying its microtubule cold-protecting effect. Indeed, since MAP6-F is not associated with the microtubules at 37°C it is washed out upon cell permeabilization. Thus, when NIH/3T3 cells were incubated and permeabilized with a Triton X-100 containing buffer at 37°C before cooling at 4°C for additional 10 min, microtubules were not protected against cold and were lost (Fig. 4*A* upper right panel). On the contrary, when cells were first pre-incubated at 4°C for 10 min to promote MAP6-F association with microtubules before permeabilization, microtubules stayed protected (Fig. 4*A* lower right panel). The amount of remaining microtubules after preincubation of the cells in various temperature conditions before permeabilization (at the same temperature) and subsequent incubation at 4°C could then be quantified by immunodetection of tubulin. We thus analyzed in similar conditions the effect of pre-incubation temperatures varying from 4°C to 37°C on MAP6-F soluble/insoluble fractionation (Fig. 4*B*) and on microtubule cold-stability (Fig. 4*C*). Results presented in Fig. 4*B* show a progressive increase in MAP6-F in the insoluble fraction and a decrease in the soluble fraction when the temperature decreased. Consistently, microtubule cold preservation increased progressively when the temperature decreased from 37°C to 4°C (Fig. 4*C*).

We next assessed in similar experiments, the kinetics of MAP6-F association with insoluble fraction and stabilization of microtubules at 4°C. As shown in Fig. 4*D*, an incubation at 4°C as short as 30 s was sufficient for maximum MAP6-F association with the insoluble fraction and this

association was reversible with apparently similar fast kinetics when cells were transferred back from 4°C to 37°C. As for the temperature dependency experiment, induction of microtubule cold-stabilization followed the localization of MAP6-F in the insoluble fraction (Fig. 4*E*). In addition, analysis of early time points showed that cold-induced stabilization of microtubules was mostly achieved within 15 s.

These results indicate that under cold exposure, MAP6-F interaction with microtubules is very fast and dynamic. This probably involves a direct effect of the temperature on one of the binding partners rather than a posttranslational modification. Furthermore, the concomitant cold exposure conditions for microtubule depolymerization (Fig. 1) and MAP6-F association with microtubules (Fig. 4) suggested that microtubules and/or MAP6-F and/or other partners involved in the interaction might undergo temperature-dependent conformational changes.

MAP6-F is a heat-stable protein that protects microtubules from cold-induced depolymerization through direct interaction via its Mc domain–In order to test whether MAP6-F by itself is capable of stabilizing microtubules and in which conditions, we carried out the purification of the MAP6-F protein as well as of its Mc domain that constitute two third of the molecule (189/306 amino acids) and has been shown to specifically protect microtubules from cold when ectopically expressed in HeLa cells (22). Both polypeptides expressed in fusion with a 6His-tag using baculovirus-insect cells system were purified to purity close to 95% (Fig. 5*A*). During the course of the purification, we also observed that MAP6-F is a heat stable protein. Indeed, contrary to most proteins that denature and precipitate at temperatures above 50°C, heating MAP6-F to 90°C for 30 min did not lead to protein aggregation (Fig. 5*B*).

Using a microtubule sedimentation assay, we analyzed the capacity of purified MAP6-F to protect *in vitro* polymerized microtubules from cold-induced depolymerization. Fig. 5*C* shows that, as expected, microtubules grown at 37°C were mostly lost when incubated at 4°C alone (lane *2*) as compared with the total amount of microtubules stabilized with taxol (lane *1*). Addition of MAP6-F just before cooling at 4°C protected microtubules from cold-induced depolymerization in a dose-dependent manner (lanes *3-5*). The same held true when heated MAP6-F was used, confirming the heat-stability of MAP6-F (lanes *7-9*). The Mc domain was also used in this assay and presented the same ability as the full-length molecule for microtubule stabilization (lanes *11-13*). It is interesting to note that the Mc domain was more soluble and did not sediment in the absence of microtubules (compare lane *14* with lanes *6* and *10*). Altogether, these results demonstrated for the first time that MAP6-F stabilizes microtubules exposed to cold *via* a direct interaction. The Mc domain is able by itself to fully recapitulate this activity and is thus the main domain involved in this function.

Characterization of the Mc domain binding to microtubules at 4°C–To further characterize the effect of the temperature on MAP6-F interaction with microtubules, we performed a titration binding curve of the Mc domain to Taxol-stabilized microtubules. Results presented in Fig. 6*A*, show that at 4°C, the Mc domain binding to 1 μM of microtubules was titrable with a binding stoechiometry of 1 mole of the Mc domain for 25 moles of tubulin dimer. The apparent affinity determined was 70 nM. On the contrary, at 37°C, no specific interaction was detected (Fig. 6*A*). Using a Mc domain concentration close to the apparent dissociation constant (Kd), we analyzed the effect of various temperatures on the Mc domain interaction with microtubules in the same conditions. Results presented in Fig 6*B* show that, as for MAP6-F association with and stabilization of microtubule in NIH/3T3 cells (Fig. 4, *B* and *C*), in vitro microtubule binding of the Mc domain progressively increases with the fall of temperature. The interaction started to be detectable at 25°C, rapidly increased between 20°C and 15°C and then was further strengthened between 15°C and 4°C.

Circular dichroism analysis of temperature-dependent conformational changes in the Mc domain–To investigate whether the temperature-associated changes in the binding affinity between the Mc domain and microtubules could be associated to conformational changes in the Mc domain, we carried out circular dichroism experiments (Fig. 7). Absorption spectra from 190 to 250 nm, obtained at different temperatures (Fig. 7*A*), indicated that the Mc domain was essentially unstructured with mainly random coiled signal (negative absorption peak near 195 nm) (27). Nevertheless, with increasing temperatures, the intensity of the negative bands at 198 nm decreased and shifted to slightly higher wavelengths while absorption at 219 nm appeared. Moreover, the presence of an

isodichroic point at 208 nm indicated a two conformational state system. In order to characterize this structuration, substraction spectra were drawn (Fig. 7*B*). The difference spectra showed the apparition with heating of negative bands at 219 nm and positive bands at 195 nm. This signal is characteristic of beta structures (28). Temperature-dependent Mc domain absorption spectra at 220 nm (Fig. 7*A insert*) indicated that the conformational change between 5°C and 80°C was linear and reversible. Altogether these data indicated that the Mc domain which contains beta structures progressively unfolded upon chilling from 37°C to 5°C.

Structural analysis of microtubules stabilized at 4°C by the Mc domain–To gain insight into the mechanisms by which MAP6-F protects microtubules from depolymerization under cold exposure, we used cryo-electron microscopy to analyze microtubules at 4°C in the absence or in the presence of the Mc domain. Growing and shrinking microtubules assume various conformations at their extremities, including sheet-like extensions and blunt ends during polymerization and outwardly curled protofilaments in disassembling conditions (29,30). As MAP6-F inhibits cold-induced microtubule disassembly, we wondered whether it could affect the global structure of microtubule ends. Microtubules were polymerized at 37°C and then incubated at 4°C with or without the Mc domain. In our conditions, we could not observe the Mc domain bound to the stabilized microtubules. The main observed differences concerned the structures of the microtubule ends that presented mostly curled depolymerizing protofilaments in the absence of the Mc domain and about 50% of blunt extremities in the presence of the Mc domain (Fig. 8). These data indicated that the Mc domain stabilized the extremities of microtubule exposed to cold. However, one would have expected a near to complete stabilization of microtubules without curled ends in the presence of the Mc domain. The remaining 50% of curled microtubule ends indicates that the microtubule stabilization is not complete and that the Mc domain might only dramatically slow down depolymerization and/or allow very slow dynamics at low temperatures.

DISCUSSION

MAP6 proteins have been shown to be essential for the stabilization of microtubules in cells at 4°C. In fibroblastic cells, the main isoform, MAP6-F, was shown to relocalize from the cytoplasm to the microtubule network upon chilling to 4°C. It has been suggested that the changes in MAP6-F binding to microtubules relied on temperature-induced changes in MAP6-F post-translational modifications (16). We show here that under cold exposure, MAP6-F recruitment to microtubules and stabilization is highly dynamic, indicating a direct effect of the temperature on the interaction. *In vitro*, purified MAP6-F can directly interact with and stabilize microtubules against cold-induced depolymerization through its Mc domain. As observed *in vivo* for MAP6-F, *in vitro* binding of the Mc domain to microtubules is temperature-dependent. The binding was very low at 37°C and increased significantly when the temperature decreased below 20°C to reach a high affinity (Kd_{app}=70nM) at 4°C. Thus, *in vivo* and *in vitro* the Mc domain of MAP6 recognizes and stabilizes microtubules as soon as the temperature drops under 20°C.

What is the structural element that regulates the interaction between microtubules and the Mc domain of MAP6? Our results reveal that lowering of temperature is accompanied by the recruitment of MAP6-F on microtubules both in cells and *in vitro*. This suggests that MAP6-F adopts a cold-dependent conformation enabling its interaction with the polymers, and/or that MAP6-F recognizes a structural feature of microtubules depolymerizing under cold exposure. Our data provide strong evidence that variations in temperatures induce conformational changes of MAP6-F. MAP6-F exhibits beta structures at 37°C and progressively unfolds as the temperature decreases, enabling its interaction with microtubules and their subsequent stabilisation. MAP6-F binding to microtubules at low temperatures could also involve the recognition of a specific feature of cold-induced depolymerizing polymers. In particular, shrinking microtubules display curled protofilaments at their ends, but we did not observe any accumulation of MAP6-F at the extremity of disassembling microtubules, neither in cells (Fig. 2 and 3) nor in purified assays (Fig. 8), suggesting that specific recognition of the outwardly curled protofilaments by MAP6-F is an unlikely mechanism. MAP6-F might associate preferentially to a cold-sensitive lattice region, although little information is available on changes occurring at low temperatures within the microtubule wall. High-resolution structures of MAP6-F and MAP6-F/microtubule complexes

will be required to visualize the Mc domain and its precise binding sites to the microtubule lattice.

How does the Mc domain of MAP6 stabilize microtubules at 4°C? As suggested above, under cold exposure, the Mc domain of MAP6 might bridge adjacent protofilaments. This, in turn, would decrease the catastrophe frequency thought to be involved in cold-induced microtubule depolymerization (9). Reinforcing lateral interactions has already been proposed to be a way of stabilizing microtubules in cold-living organisms (12). Such a mechanism is reminiscent of the doublecortin microtubule-stabilization mode at 37°C (31). Doublecortin is an anti-catastrophe factor that stabilizes microtubules by linking adjacent protofilaments and counteracting their outward bending in depolymerizing microtubules (32). The analysis of the Mc domain effects on microtubule dynamics at low temperature should be very informative but such experiments which require a controlled cold environment are still technically challenging.

A link between the Mc domain structure and MAP6 aggregation in human pathology? During our in vitro studies we discovered that MAP6-F is a weakly structured molecule as revealed by its heat-stability, a feature shared by other MAPs such as MAP1, MAP2 and Tau (33). The folding of MAP6F into beta structures represents a peculiar behavior already reported for the Tau protein (34). These beta structures have been implicated in the formation of pathologic amyloid aggregates (35) and beta structures of MAP6 might be implicated in the aggregation of MAP6 in Lewis bodies during amyotrophic lateral sclerosis (36).

A physiological function for MAP6 stabilization of microtubules under cold exposure? In HeLa cells, that do not express MAP6 proteins, microtubules depolymerized in a temperature-dependent manner as soon as the temperature decreased below 20°C with virtually no microtubules left at 4°C. On the contrary, in MAP6-containing NIH/3T3 cells, 80% of microtubules were preserved upon cold exposure from 20°C to 4°C. In more physiological conditions, MAP6 of $MEF^{+/+}$ allowed to preserve about 80% of microtubules at 15°C and 30% at temperatures below 10°C. In animals, such low temperatures could be achieved during episodes of torpor or hibernation and MAP6 could be required to preserve a minimal level of microtubules in such challenging conditions. In this study we considered the whole Mc domain without analyzing the contribution of each individual repeat. However, one can speculate that the composition in repeats of the Mc domain would determine the strength of the cold response. Along this line, we found a relatively good correlation between the number of repeats (from 1 to 9) in the Mc domain of mammals and the ability of the animals to hibernate or to make torpor. For example, almost all genome-sequenced rodents (house mice, Norway rat, thirteen-lined ground squirrel) which exhibit MAP6 with 3 to 9 Mc repeats are able to hibernate/torpor, whereas the naked mole rat which exhibits only one repeat is very sensitive to cold exposure (main cause of lethality).

Also, in primates, only the lemurian branch which contains several Mc repeats (3 to 6 for small-eared galago and grey mouse lemur) can enter torpor whereas all other primates including human, Sumatran ourangutan, chimpanzee, gorilla, Rhesus monkey and Hamadryas baboon do not enter torpor and express MAP6 containing only one repeat. In human, MAP6 stabilization of microtubules can still be useful during accidental hypothermic episodes or even during perioperative hypothermia following anesthesia.

In conclusion, the Mc domain of MAP6 behaves as a sensor of temperature able to protect microtubules from temperature variations. How microtubule stabilization upon temperature reduction is involved and whether it is crucial to adapt cold-dependent cell responses such as metabolic changes are exciting questions.

REFERENCES

1. Akhmanova, A., and Steinmetz, M. O. (2008) Tracking the ends: a dynamic protein network controls the fate of microtubule tips. *Nat Rev Mol Cell Biol* **9**, 309-322
2. Howard, J., and Hyman, A. A. (2009) Growth, fluctuation and switching at microtubule plus ends. *Nat Rev Mol Cell Biol* **10**, 569-574
3. Nogales, E., and Wang, H. W. (2006) Structural intermediates in microtubule assembly and disassembly: how and why? *Curr Opin Cell Biol* **18**, 179-184
4. Wade, R. H. (2009) On and around microtubules: an overview. *Mol Biotechnol* **43**, 177-191
5. Lee, J. C., and Timasheff, S. N. (1977) In vitro reconstitution of calf brain microtubules: effects of solution variables. *Biochemistry* **16**, 1754-1764
6. Olmsted, J. B., and Borisy, G. G. (1975) Ionic and nucleotide requirements for microtubule polymerization in vitro. *Biochemistry* **14**, 2996-3005
7. Regula, C. S., Pfeiffer, J. R., and Berlin, R. D. (1981) Microtubule assembly and disassembly at alkaline pH. *The Journal of cell biology* **89**, 45-53
8. Schilstra, M. J., Bayley, P. M., and Martin, S. R. (1991) The effect of solution composition on microtubule dynamic instability. *Biochem J* **277 (Pt 3)**, 839-847
9. Fygenson, D. K., Braun, E., and Libchaber, A. (1994) Phase diagram of microtubules. *Phys Rev E Stat Phys Plasmas Fluids Relat Interdiscip Topics* **50**, 1579-1588
10. Modig, C., Wallin, M., and Olsson, P. E. (2000) Expression of cold-adapted beta-tubulins confer cold-tolerance to human cellular microtubules. *Biochem Biophys Res Commun* **269**, 787-791
11. Detrich, H. W., 3rd. (1997) Microtubule assembly in cold-adapted organisms: functional properties and structural adaptations of tubulins from antarctic fishes. *Comp Biochem Physiol A Physiol* **118**, 501-513
12. Detrich, H. W., 3rd, Parker, S. K., Williams, R. C., Jr., Nogales, E., and Downing, K. H. (2000) Cold adaptation of microtubule assembly and dynamics. Structural interpretation of primary sequence changes present in the alpha- and beta-tubulins of Antarctic fishes. *J Biol Chem* **275**, 37038-37047
13. Geiser, F. (1988) Reduction of metabolism during hibernation and daily torpor in mammals and birds: temperature effect or physiological inhibition? *J Comp Physiol B* **158**, 25-37
14. Heldmaier, G., Ortmann, S., and Elvert, R. (2004) Natural hypometabolism during hibernation and daily torpor in mammals. *Respir Physiol Neurobiol* **141**, 317-329
15. Andrieux, A., Salin, P. A., Vernet, M., Kujala, P., Baratier, J., Gory-Faure, S., Bosc, C., Pointu, H., Proietto, D., Schweitzer, A., Denarier, E., Klumperman, J., and Job, D. (2002) The suppression of brain cold-stable microtubules in mice induces synaptic defects associated with neuroleptic-sensitive behavioral disorders. *Genes Dev* **16**, 2350-2364
16. Denarier, E., Fourest-Lieuvin, A., Bosc, C., Pirollet, F., Chapel, A., Margolis, R. L., and Job, D. (1998) Nonneuronal isoforms of STOP protein are responsible for microtubule cold stability in mammalian fibroblasts. *Proc Natl Acad Sci U S A* **95**, 6055-6060
17. Bosc, C., Andrieux, A., and Job, D. (2003) STOP proteins. *Biochemistry* **42**, 12125-12132
18. Aguezzoul, M., Andrieux, A., and Denarier, E. (2003) Overlap of promoter and coding sequences in the mouse STOP gene (Mtap6). *Genomics* **81**, 623-627
19. Galiano, M. R., Bosc, C., Schweitzer, A., Andrieux, A., Job, D., and Hallak, M. E. (2004) Astrocytes and oligodendrocytes express different STOP protein isoforms. *J Neurosci Res* **78**, 329-337
20. Guillaud, L., Bosc, C., Fourest-Lieuvin, A., Denarier, E., Pirollet, F., Lafanechere, L., and Job, D. (1998) STOP proteins are responsible for the high degree of microtubule stabilization observed in neuronal cells. *The Journal of cell biology* **142**, 167-179
21. Ochoa, C. D., Stevens, T., and Balczon, R. (2010) Cold exposure reveals two populations of microtubules in pulmonary endothelia. *Am J Physiol Lung Cell Mol Physiol* **300**, L132-138

22. Bosc, C., Frank, R., Denarier, E., Ronjat, M., Schweitzer, A., Wehland, J., and Job, D. (2001) Identification of novel bifunctional calmodulin-binding and microtubule-stabilizing motifs in STOP proteins. *J Biol Chem* **276**, 30904-30913
23. Lieuvin, A., Labbe, J. C., Doree, M., and Job, D. (1994) Intrinsic microtubule stability in interphase cells. *The Journal of cell biology* **124**, 985-996
24. Erck, C., Peris, L., Andrieux, A., Meissirel, C., Gruber, A. D., Vernet, M., Schweitzer, A., Saoudi, Y., Pointu, H., Bosc, C., Salin, P. A., Job, D., and Wehland, J. (2005) A vital role of tubulin-tyrosine-ligase for neuronal organization. *Proc Natl Acad Sci U S A* **102**, 7853-7858
25. Schneider, C. A., Rasband, W. S., and Eliceiri, K. W. (2012) NIH Image to ImageJ: 25 years of image analysis. *Nat Meth* **9**, 671-675
26. Paturle-Lafanechere, L., Edde, B., Denoulet, P., Van Dorsselaer, A., Mazarguil, H., Le Caer, J. P., Wehland, J., and Job, D. (1991) Characterization of a major brain tubulin variant which cannot be tyrosinated. *Biochemistry* **30**, 10523-10528
27. Venyaminov, S., Baikalov, I. A., Shen, Z. M., Wu, C. S., and Yang, J. T. (1993) Circular dichroic analysis of denatured proteins: inclusion of denatured proteins in the reference set. *Anal Biochem* **214**, 17-24
28. Greenfield, N., and Fasman, G. D. (1969) Computed circular dichroism spectra for the evaluation of protein conformation. *Biochemistry* **8**, 4108-4116
29. Arnal, I., Karsenti, E., and Hyman, A. A. (2000) Structural transitions at microtubule ends correlate with their dynamic properties in Xenopus egg extracts. *The Journal of cell biology* **149**, 767-774
30. Chretien, D., Fuller, S. D., and Karsenti, E. (1995) Structure of growing microtubule ends: two-dimensional sheets close into tubes at variable rates. *The Journal of cell biology* **129**, 1311-1328
31. Moores, C. A., Perderiset, M., Francis, F., Chelly, J., Houdusse, A., and Milligan, R. A. (2004) Mechanism of microtubule stabilization by doublecortin. *Mol Cell* **14**, 833-839
32. Moores, C. A., Perderiset, M., Kappeler, C., Kain, S., Drummond, D., Perkins, S. J., Chelly, J., Cross, R., Houdusse, A., and Francis, F. (2006) Distinct roles of doublecortin modulating the microtubule cytoskeleton. *Embo J* **25**, 4448-4457
33. Vera, J. C., Rivas, C. I., and Maccioni, R. B. (1988) Heat-stable microtubule protein MAP-1 binds to microtubules and induces microtubule assembly. *FEBS Lett* **232**, 159-162
34. von Bergen, M., Friedhoff, P., Biernat, J., Heberle, J., Mandelkow, E. M., and Mandelkow, E. (2000) Assembly of tau protein into Alzheimer paired helical filaments depends on a local sequence motif ((306)VQIVYK(311)) forming beta structure. *Proc Natl Acad Sci U S A* **97**, 5129-5134
35. Mukrasch, M. D., Biernat, J., von Bergen, M., Griesinger, C., Mandelkow, E., and Zweckstetter, M. (2005) Sites of tau important for aggregation populate {beta}-structure and bind to microtubules and polyanions. *J Biol Chem* **280**, 24978-24986
36. Letournel, F., Bocquet, A., Dubas, F., Barthelaix, A., and Eyer, J. (2003) Stable tubule only polypeptides (STOP) proteins co-aggregate with spheroid neurofilaments in amyotrophic lateral sclerosis. *J Neuropathol Exp Neurol* **62**, 1211-1219

Acknowledgment–We are grateful to D. Job for helpful discussions on the work and to L. Aubry, J. Brocard, F. Costagliola, and J.C, Deloulme for critical reading of the manuscript.

FOOTNOTES

This work was supported by INSERM, CEA, University Joseph Fourier and the French National Research Agency awards 2010Blan120201 CBioS to AA. MB is the recipient of the Roche Pharmaceutic RPF program (AA team and F Hoffmann-La Roche Ltd, Basel, Switzerland).
[§]To whom correspondence should be addressed: Christian Delphin, Inserm U836, Equipe 1, Bâtiment Edmond J. Safra, Université Joseph Fourier, Site Santé à La Tronche , BP 170, 38042 GRENOBLE Cedex 9 – France, Tel: (33)-456-520-539; Fax: (33)-456-520-657; E-Mail: christian.delphin@ujf-grenoble.fr
The abbreviations used are: GTP, guanoside triphosphate; DMEM, Dulbecco's modified Eagle medium; MEF, mouse embryonic fibroblasts; PBS, Phosphate buffered saline; HRP, horseradish peroxidase; EGTA, ethylene glycol tetraacetic acid; DTT, dithiothreitol; HEPES, 4-(2-hydroxyethyl)-1-piperazineethanesulfonic acid; PIPES, piperazine-N,N′-bis(2-ethanesulfonic acid); SDS-PAGE, sodium dodecyl sulfate polyacrylamide gel electrophoresis.

FIGURE LEGENDS

FIGURE 1. MAP6-F protects fibroblastic microtubules from temperature- and time-dependent cold-induced depolymerization. *A*, Imunofluorescence analysis of microtubules of NIH/3T3 cells, HeLa cells, $MEF^{+/+}$ and $MEF^{-/-}$ exposed to the indicated temperature. *B* and *C*, Quantification of microtubule surface in immunofluorescence experiments as shown in *A* for each cell line (NIH/3T3 and HeLa in *B*, $MEF^{+/+}$ and $MEF^{-/-}$ in *C*). *D*, NIH/3T3, HeLa, $MEF^{+/+}$ and $MEF^{-/-}$ cell extracts were normalized for their content in tubulin and then analyzed for the expression of MAP6-F by Western blot. * Indicates minor MAP6 isoforms (16,19). *E*, Quantification of microtubules remaining in HeLa cells after incubation for the indicated time at 4°C or 15°C. In *B*, *C* and *E*, data represent mean ± s.e.m ($n \geq 12$) and are expressed as a percentage of the signal obtained without cold treatment (37°C).

FIGURE 2. Cold-induced association of MAP6 with the microtubule network in MEF. $MEF^{+/+}$ or $MEF^{-/-}$ were either kept at 37°C or incubated at 4°C for 30 min as indicated. Cells were then permeabilized with OPT at the incubation temperature, fixed and processed for immunodetection of tubulin (green) or MAP6-F (red).

FIGURE 3. Cooling cells from 37°C to 15°C induces a progressive accumulation of MAP6-F-mCherry on microtubule network in HeLa cells. HeLa cells overexpressing MAP6-F fused to mCherry were placed in a perfusion chamber at 37°C. Cell culture medium was progressively cooled from 37°C to 15°C during the course of the experiment (15 min, 30 s). Upper panels are recorded images of MAP6-F-mCherry at the indicated time (min:s). Lower panels are enlargements (3x) of part of the images indicated by white squares.

FIGURE 4. MAP6-F association with microtubules and stabilization of microtubules are fast and temperature-dependent. *A*, NIH/3T3 cells at 37°C (*upper lane*) or incubated at 4°C (*lower lane*), were permeabilized (TX100) and either directly fixed (*left*) or further incubated for 10 min at 37°C (*upper middle*) or at 4°C (*upper* and *lower right*) before microtubule immunodetection. *B*, Western blot analysis of MAP6-F present in soluble (*S*) or insoluble (*I*) fractions of NIH/3T3 cells exposed to the indicated temperature. *C*, Quantification by immunofluorescence of the remaining microtubules in NIH/3T3 cells pre-incubated and permeabilized at the indicated temperature, and then further incubated at 4°C. Data represent mean ± s.e.m ($n \geq 12$) and are expressed as a percentage of the signal obtained without cold treatment (37°C). *D*, and *E*, NIH/3T3 cells were treated as in *B* and *C* respectively, except that the cell incubation and permeabilization temperatures were switched from

37°C to 4°C and then from 4°C back to 37°C. MAP6-F solubility (*D*) and subsequent microtubule cold stabilization at 4°C (*E*) were analyzed at the indicated time course.

FIGURE 5. MAP6-F is a heat stable protein that stabilizes microtubules *in vitro* through interaction with its Mc domain. *A*, Coomassie blue stained SDS-PAGE gel of the purification products of MAP6-F and the Mc domain expressed as His-tagged proteins in insect cells. *B*, Solubility analysis of purified MAP6-F at 4°C or after heating for 30 min at 90°C. Proteins in the 100,000 x *g* pellet (*P*) or supernatant (*S*) were analysed in Coomassie blue stained SDS-PAGE gel. *T*: total. *C*, Microtubule cold-stabilization activity of MAP6-F, heated MAP6-F, and the Mc domain. Microtubules were grown from pure tubulin *in vitro*, mixed with either taxol (60 μM) or increasing concentration of MAP6-F, 90°C-treated MAP6-F, or with the Mc repeat domain as indicated and then incubated on ice for 10 min. Cold-resistant microtubules were isolated by centrifugation and the pellets were analyzed by SDS-PAGE and Coomassie blue staining.

FIGURE 6. *In vitro* analysis of temperature-dependent binding of the MAP6 Mc domain with taxol-stabilized microtubules. *A*, Microtubules were grown at 37°C from 60 μM of pure tubulin, stabilized with Taxol and diluted to 1 μM in the final binding reaction mix. The Mc domain was added at increasing concentrations and incubated at 4°C or 37°C for 10 min. Microtubules were isolated by centrifugation and the associated Mc domain was quantified by Western blot using Chemidoc apparatus, ImageJ and Excel softwares. 4°C and 37°C controls (*Ctrl*) are the amount of the Mc domain pelleted in the absence of microtubules. *B*, Lineweaver-Burk plot analysis of the data shown in *A* gave 70 nM as the apparent dissociation constant (Kd_{app}) for the binding of the Mc domain to microtubules at 4°C. *C,* the Mc domain (50 nM) binding to microtubules was analyzed as in *A* at the indicated temperatures.

FIGURE 7. Temperature induces secondary structure changes in the Mc domain of MAP6. *A*, Circular dichroism spectra at 5°C showed a clear minimum for the spectrum at 198 nm, indicating a mostly random coiled structure. This minimum is shifted with increasing temperature towards higher wavelengths and a minimum at 219 nm appears. This indicates an increase in structuration. In the insert, the structuration has been monitored at 220 nm from 5°C to 85°C as indicated by the black arrow. The folding reversibility from 85°C to 5°C is indicated by the open arrow. The isodichroic point at 208 nm suggests a two-state system characterizing the secondary structure of the Mc domain. *B*, Difference CD spectra from *A*. The substraction of the CD spectrum at 5°C from CD spectra at 10°C, 20°C, 40°C and 70°C gave the structuration gain during the temperature titration. The spectra obtained correspond to beta-sheet conformation.

FIGURE 8. Microtubule cold-stabilization by the Mc domain is associated with an increase of blunt-ended microtubules. Microtubules were grown from 80 μM of pure tubulin at 37°C, mixed at a final concentration of 55 μM with buffer alone (*Ctrl*) or with 5.5 μM final of the Mc domain (*Mc*). After 10 min at 37°C, microtubules were chilled on ice for 1 min to allow partial depolymerization of microtubules alone or for 20 min for the Mc domain stabilized microtubules. Microtubules were loaded on grids, frozen in liquid ethane and observed by cryo-electron microscopy. *A*, Pictures and schematic representations of microtubule curled and blunt ends. *B,* Quantitative analysis of the proportion of blunt versus curled ends in control condition or in the presence of the Mc domain.

Figure 1

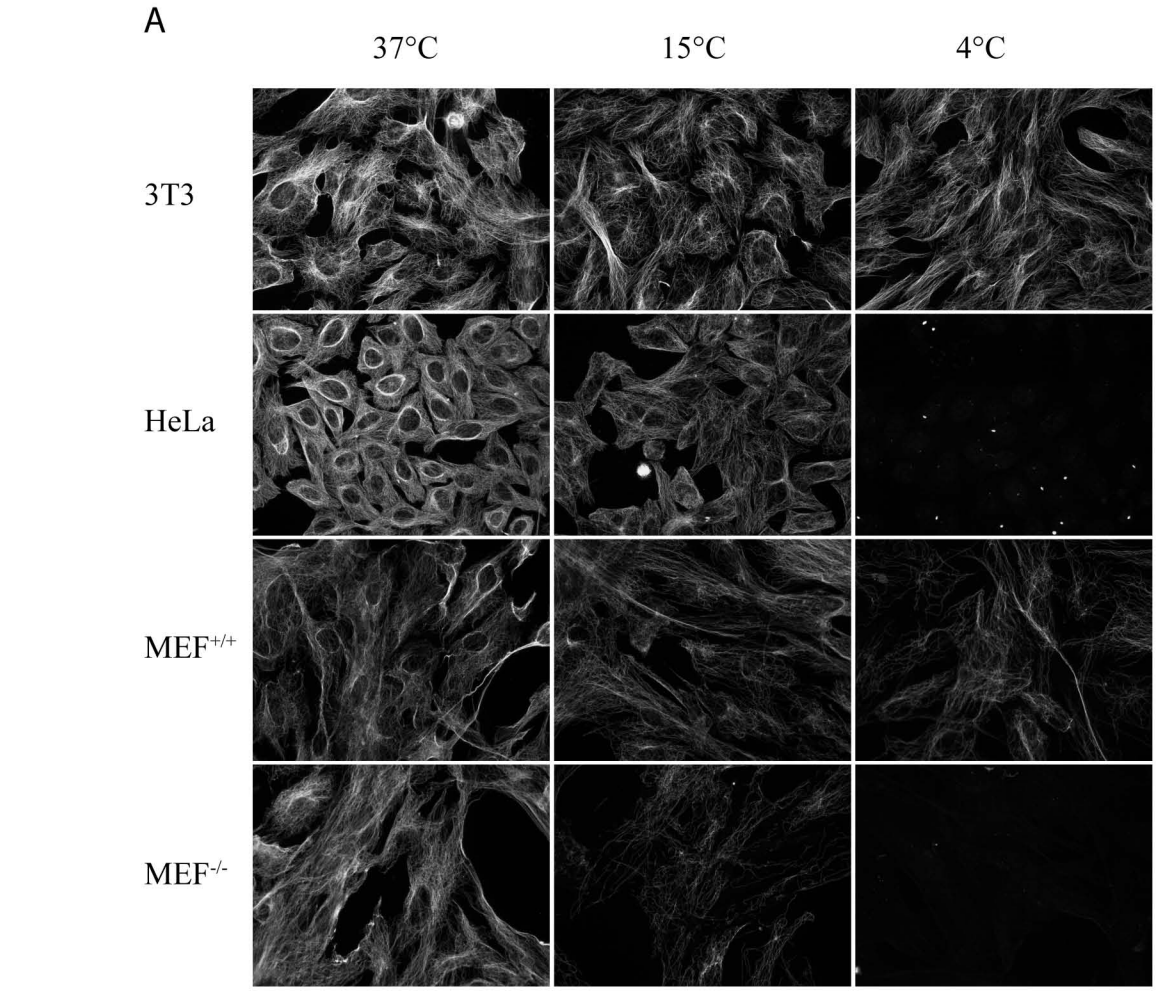
A
37°C
15°C
4°C
3T3
HeLa
MEF+/+
MEF-/-

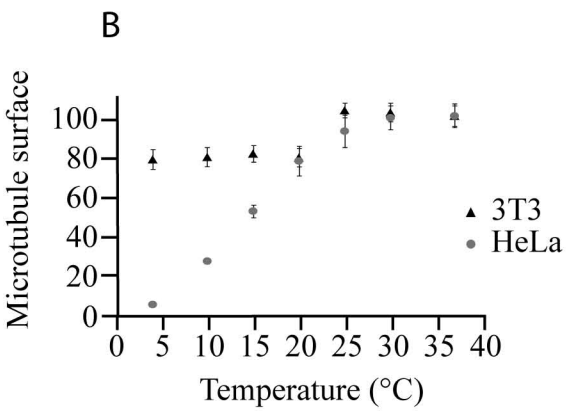
B
Microtubule surface
Temperature (°C)
3T3
HeLa

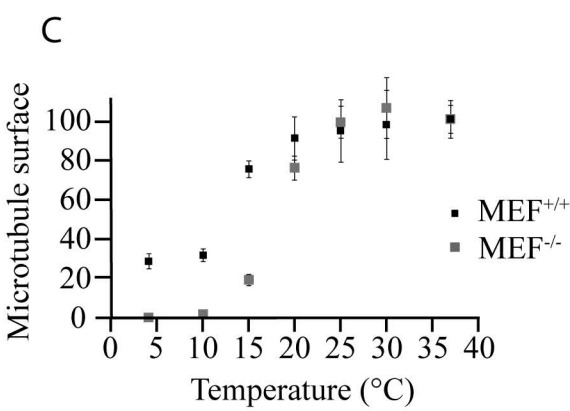
C
Microtubule surface
Temperature (°C)
MEF+/+
MEF-/-

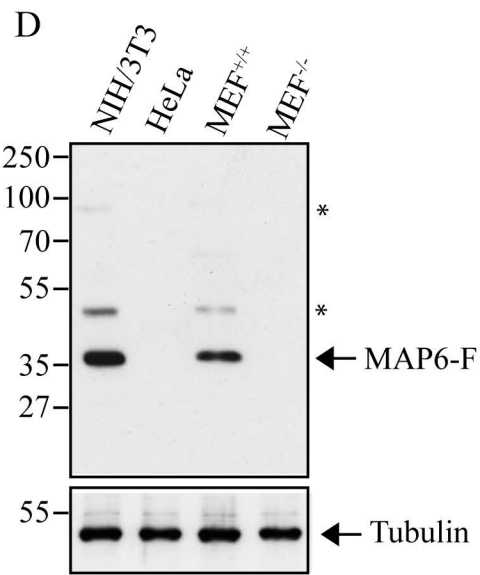
D
NIH/3T3
HeLa
MEF+/+
MEF-/-
MAP6-F
Tubulin

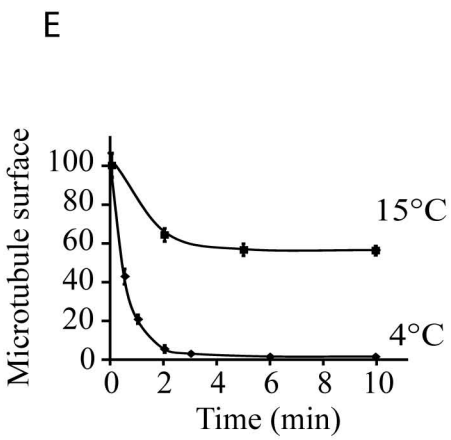
E
Microtubule surface
Time (min)
15°C
4°C

Figure 2

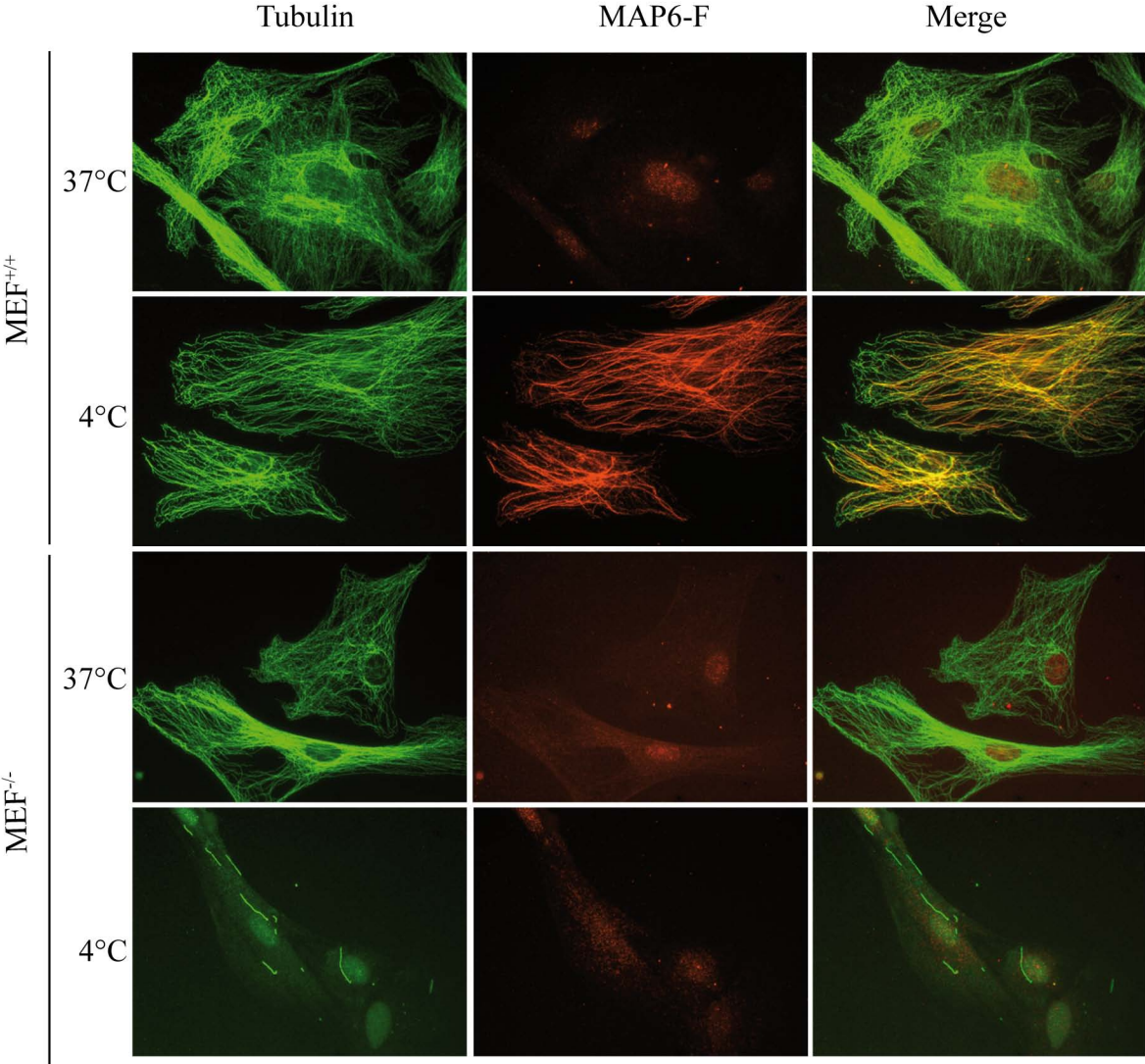

Figure 3

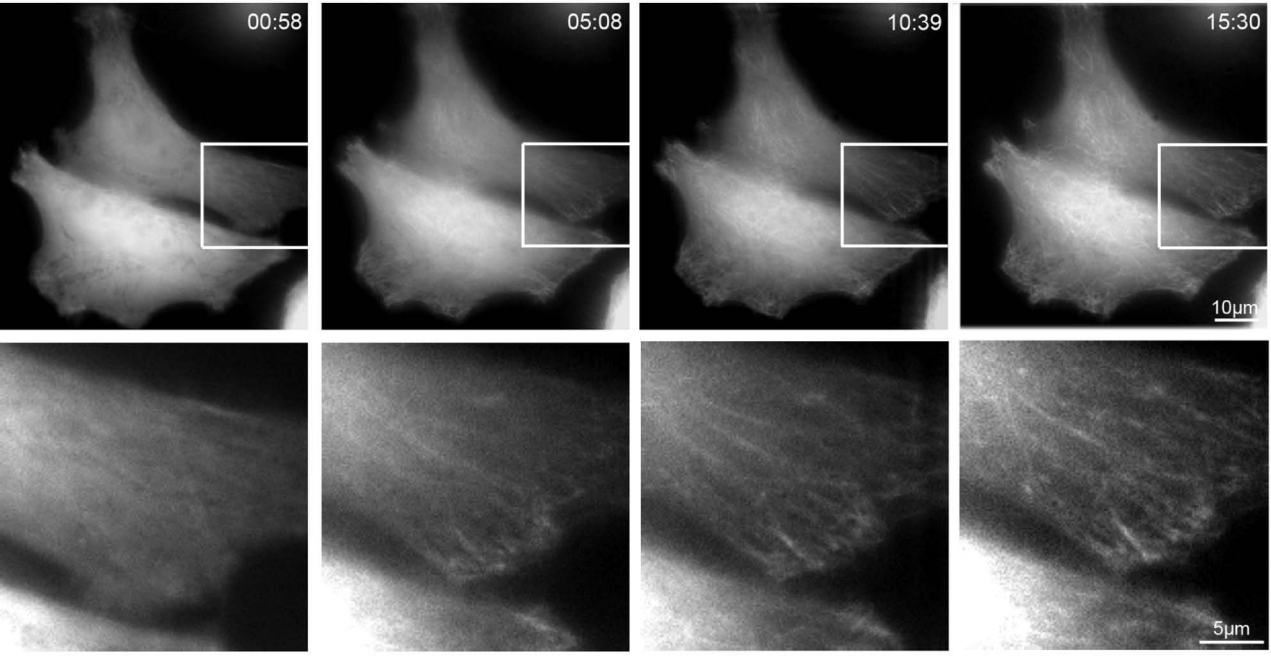

Figure 4

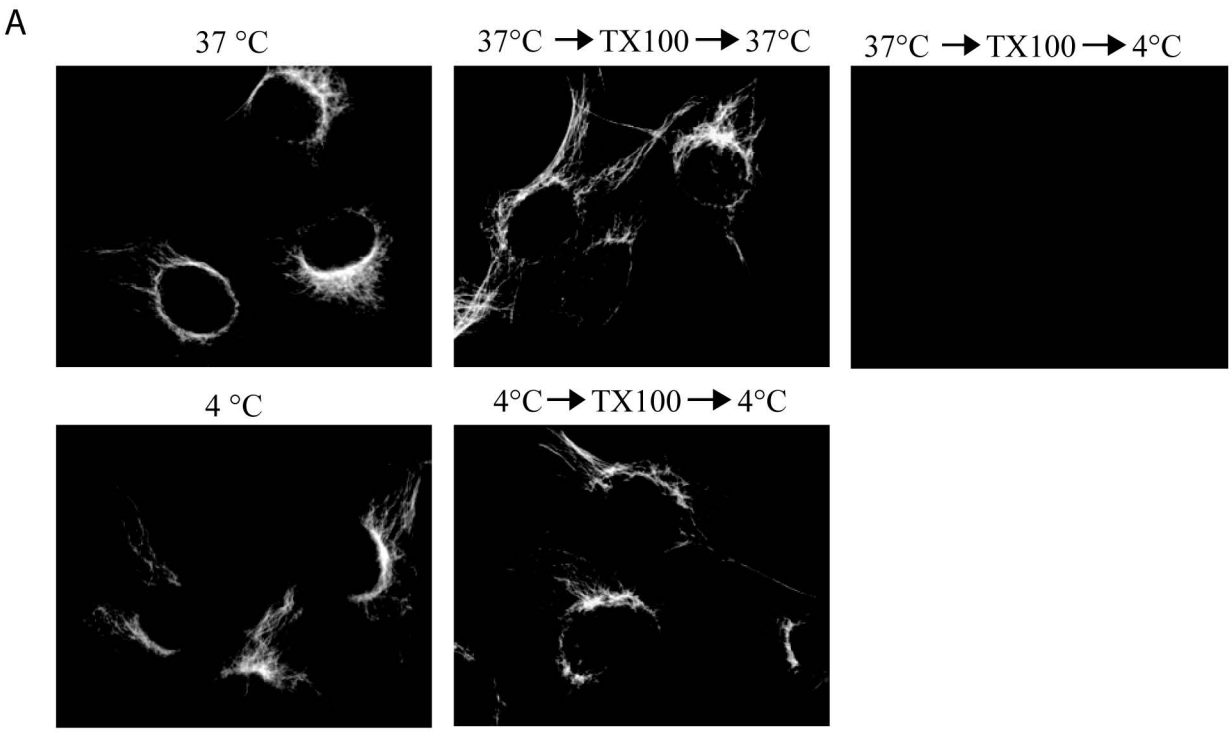
A
37 °C
37°C → TX100 → 37°C
37°C → TX100 → 4°C
4 °C
4°C → TX100 → 4°C

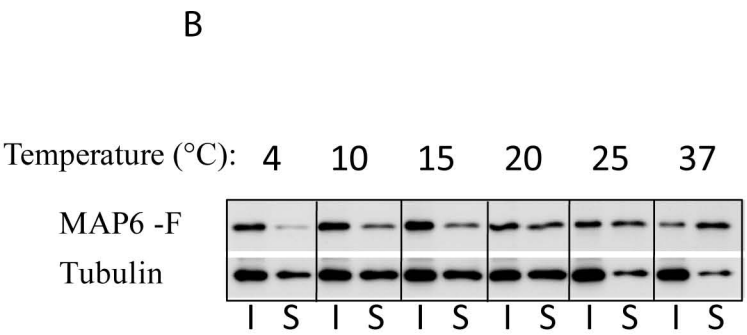
B
Temperature (°C): 4 10 15 20 25 37
MAP6 -F
Tubulin
I S I S I S I S I S I S

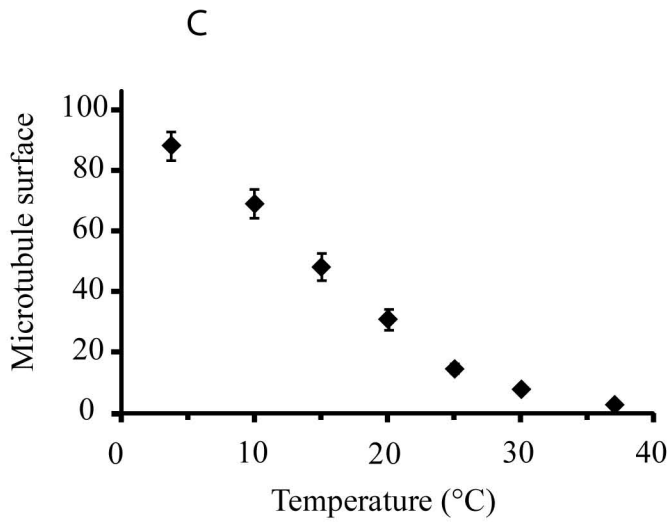
C
Microtubule surface
100
80
60
40
20
0
0 10 20 30 40
Temperature (°C)

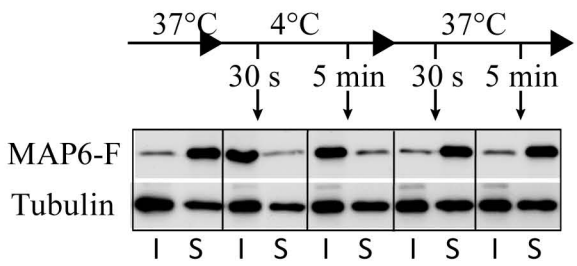
D
37°C 4°C 37°C
30 s 5 min 30 s 5 min
MAP6-F
Tubulin
I S I S I S I S I S

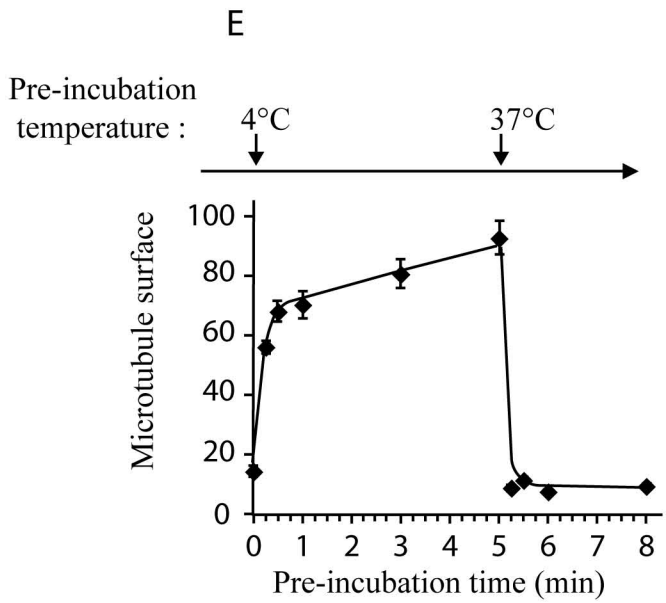
E
Pre-incubation temperature :
4°C
37°C
Microtubule surface
100
80
60
40
20
0
0 1 2 3 4 5 6 7 8
Pre-incubation time (min)

Figure 5

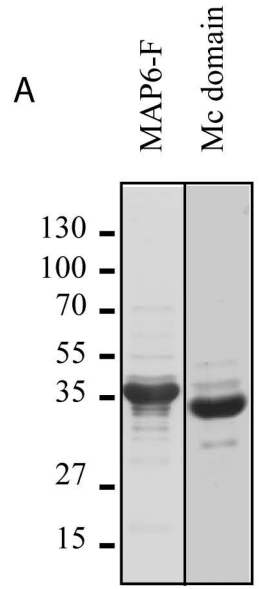

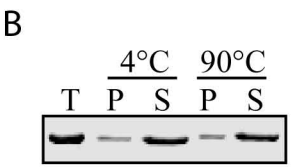

C

Microtubules (30 µM)	+	+	+	+	+		+	+	+		+	+	+	
Taxol	+													
MAP6-F (µM)			0.5	1.5	5	5								
Heated MAP6-F (µM)							0.5	1.5	5	5				
Mc domain (µM)											0.5	1.5	5	5

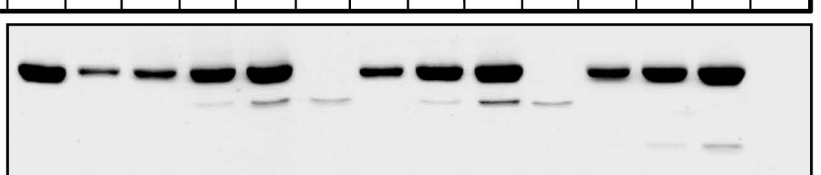

Figure 6

A

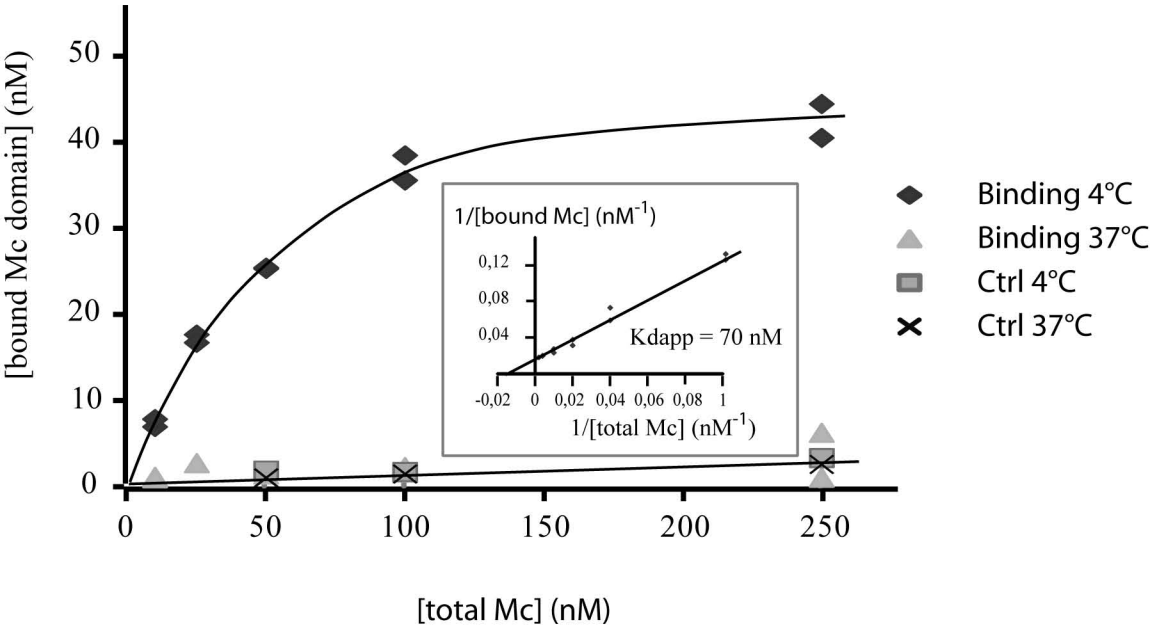
[bound Mc domain] (nM)
50
40
30
20
10
0
0
50
100
150
200
250
[total Mc] (nM)
1/[bound Mc] (nM-1)
0,12
0,08
0,04
Kdapp = 70 nM
-0,02
0
0,02
0,04
0,06
0,08
1
1/[total Mc] (nM-1)
Binding 4°C
Binding 37°C
Ctrl 4°C
Ctrl 37°C

B

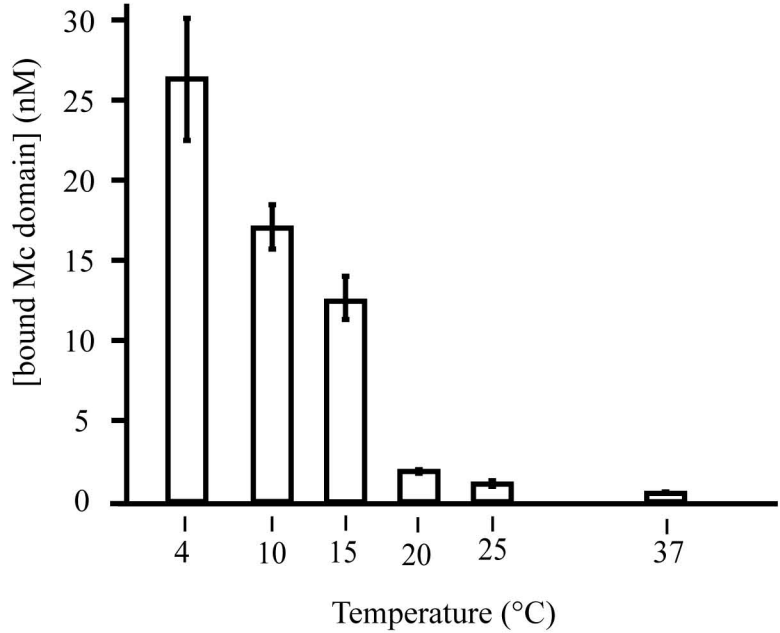
[bound Mc domain] (nM)
30
25
20
15
10
5
0
4
10
15
20
25
37
Temperature (°C)

Figure 7

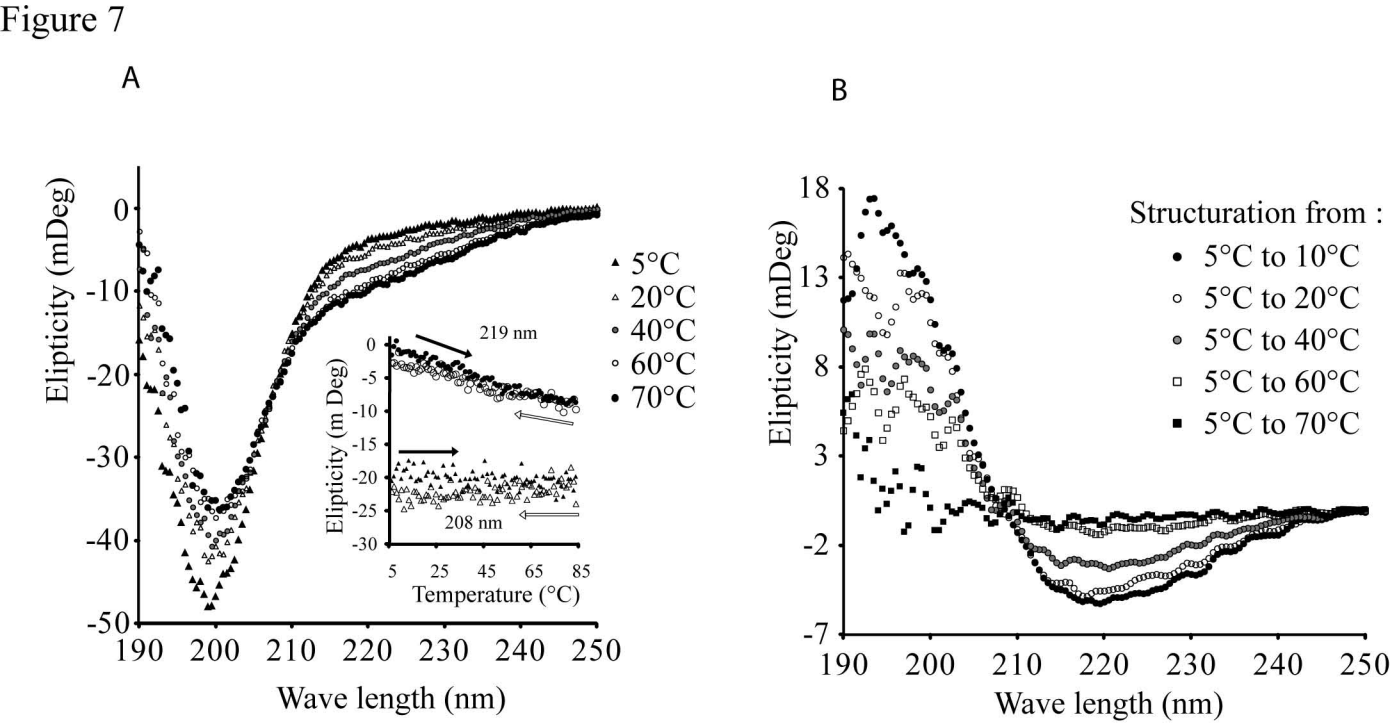
A
Elipticity (mDeg)
0
-10
-20
-30
-40
-50
190
200
210
220
230
240
250
Wave length (nm)
5°C
20°C
40°C
60°C
70°C
219 nm
208 nm
Elipticity (m Deg)
0
-5
-10
-15
-20
-25
-30
5
25
45
65
85
Temperature (°C)
B
Elipticity (mDeg)
18
13
8
3
-2
-7
190
200
210
220
230
240
250
Wave length (nm)
Structuration from :
5°C to 10°C
5°C to 20°C
5°C to 40°C
5°C to 60°C
5°C to 70°C

Figure 8

A

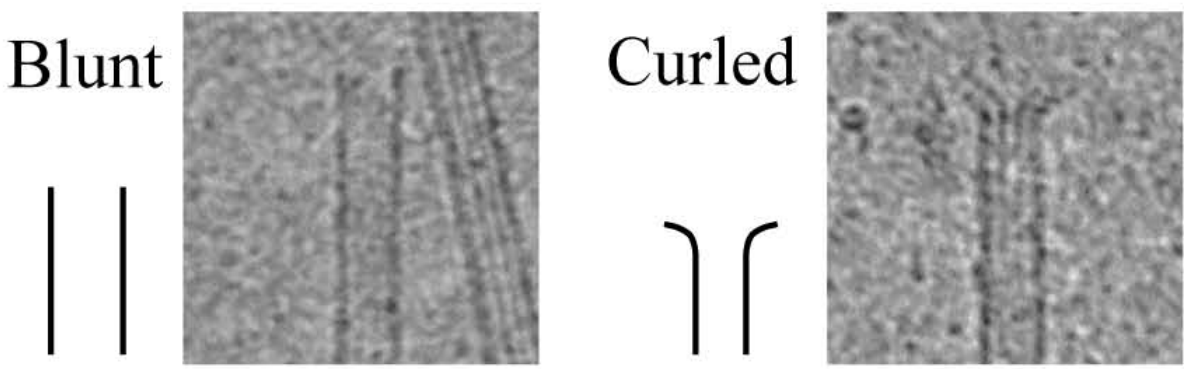
Blunt
Curled

B

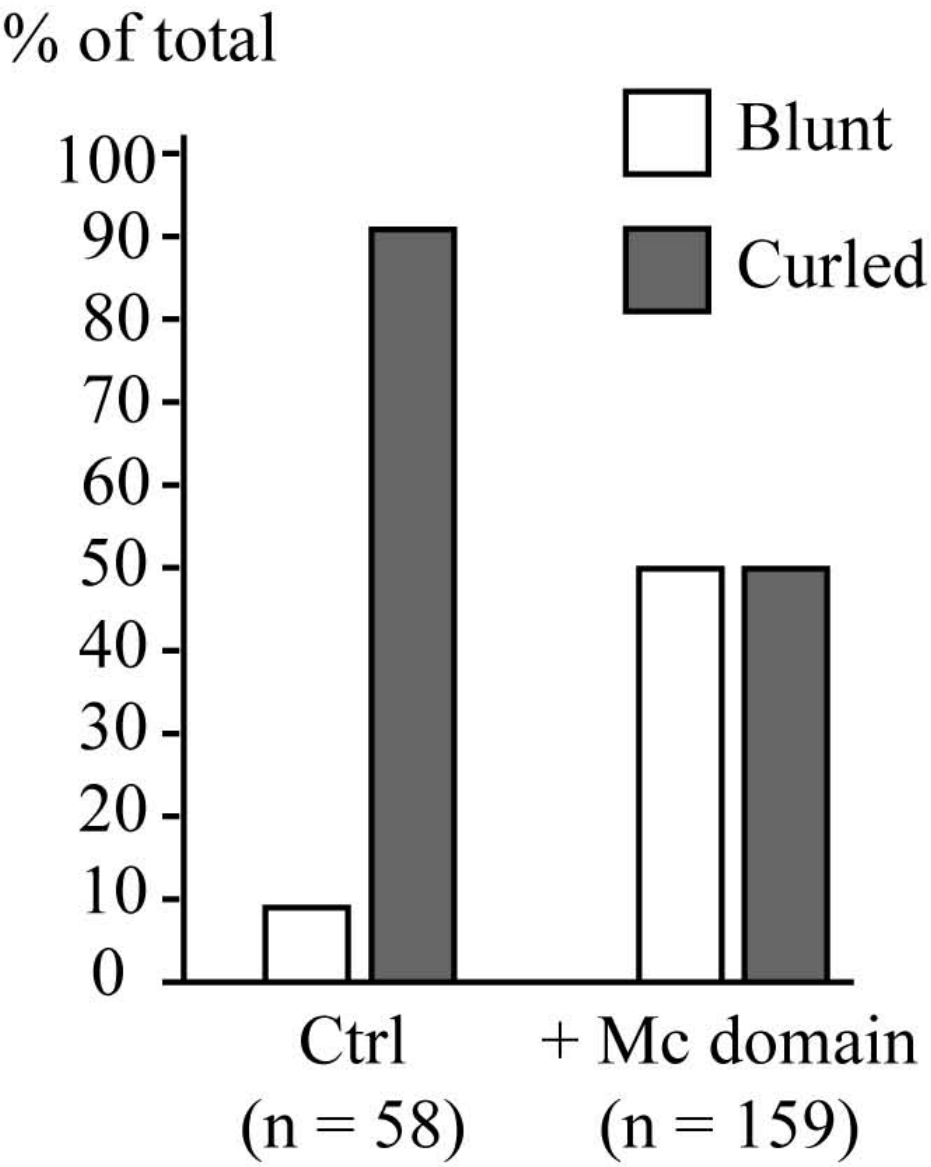
% of total
Blunt
Curled
100
90
80
70
60
50
40
30
20
10
0
Ctrl
(n = 58)
+ Mc domain
(n = 159)